INHOMOGENEOUS FIELD BREAKDOWN IN GIS THE PREDICTION OF BREAKDOWN PROBABILITIES AND VOLTAGES*

Part III: Discharge Development in SF_6 and Computer Model of Breakdown

N. Wiegart, L. Niemeyer, F. Pinnekamp, BBC Research Laboratory, Switzerland
W. Boeck, J. Kindersberger, Technical University of Munich, West Germany
R. Morrow, CSIRO, Australia
W. Zaengl, M. Zwicky, ETH Zurich, Switzerland
I. Gallimberti, University of Padua, Italy
S.A. Boggs, Ontario Hydro, Canada

Abstract Extensive investigations into various phases of discharge development in SF_6 (corona formation, streamer to leader transition, leader propagation) are summarized in this paper, with the goal of familiarizing the reader with the theoretical and empirical basis of a quantitative model for SF_6 breakdown, including breakdown in highly inhomogeneous fields. The quantitative predictive capability of this model is tested for a number of examples, which demonstrate the correct prediction of geometry and pressure dependencies of the breakdown voltage. Combined with the modified volume time "law", the breakdown model becomes a valuable tool for the power engineer, capable of predicting statistical breakdown characteristics for a wide range of gap geometries and positive voltage waveforms as a function of pressure. At present, the model does not cover negative polarity waveforms and becomes increasingly inaccurate as the waveform risetime increases over about 10 μs. Future research is planned to address both of these limitations. Practical applications are outlined.

INTRODUCTION

The purpose of this third paper on inhomogeneous field breakdown in GIS is to summarize the results of experimental and theoretical investigations of the different stages of discharge development in SF_6 under positive impulse stress. In order not to obscure technical relevance, details have been omitted where they do not contribute to the understanding of physical processes. The interested reader is referred to the comprehensive final report of CEA Contract 153 T 310 [1]. However, more recent results [2,3] have led to the clarification of some important points.

The important issue of discharge initiation has been discussed in great detail in the second paper. Here, the processes following the production of initial electrons will be described in the order in which they occur physically, i.e., corona development followed by leader inception and leader propagation up to breakdown. Knowledge of discharge processes is used to establish a numerical breakdown model which is largely based on physical theories but is simplified to obtain an optimum compromise between accuracy and computational effort.

The last two sections will probably be the most interesting for the power engineer, as they demonstrate the predictive capability of the model and give examples of practical applications.

*Research sponsored, in part, by the Canadian Electrical Association.

87 WM 192-8 A paper recommended and approved by the IEEE Substations Committee of the IEEE Power Engineering Society for presentation at the IEEE/PES 1987 Winter Meeting, New Orleans, Louisiana, February 1 - 6, 1987. Manuscript submitted July 8, 1986; made available for printing November 26, 1986.

DEVELOPMENT OF THE IMPULSE CORONA

"Corona" is a term used so frequently and for such a wide range of partial discharge or prebreakdown phenomena that a clear definition of what is meant in the context of this study must be provided. As only the case of fast rising waveforms is discussed, the term corona will denote a burst of streamers developing concurrently in the virgin gas (sometimes referred to as "impulse corona" as opposed to "repetitive corona"). Note that this definition excludes glow corona, which is unlikely to appear in the parameter range of interest for practical applications.

Unfortunately, some confusion also exists in the application of the term "streamer", which is used for almost any type of channel-like discharge feature (e.g., the "secondary" streamer that should better be termed "leader"). Here a "streamer" is an ionization wave restricted to a channel of small radius which develops in the virgin gas and which is characterized by a large electric field at its leading edge (caused by space charge) and a low conductivity. This definition still encompasses a multitude of physical mechanisms depending on the properties of the gas. For example, we will demonstrate that streamers in air and SF_6 have very little in common.

From optical observations of SF_6 coronae over a wide range of voltage, pressure, and gap geometry, we have found that corona extension and corona charge obey simple electrostatic laws which can be explained unambiguously in terms of the physical conditions for the existence of a streamer in SF_6. Figure 1 shows a typical example of a corona Schlieren photograph, obtained with a rod to plane gap. The Schlieren technique has the advantage over simple self-luminosity streak or framing records of displaying density gradients and thereby revealing details of corona structure. A clear distinction can be made between a practically homogeneous zone close to the electrode and a filamentary feature further out.

Figure 1 Corona Schlieren Photograph of a rod plane gap with 1 mm rod diameter and 65 mm gap spacing for 300 kV and 1 bar SF_6 pressure.

As yet, the theoretical models of streamer propagation in SF_6 still suffer from severe restrictions and do not allow a complete numerical simulation of corona formation. They have, however, predicted that a streamer track in SF_6 is necessarily characterized by an electric field very close to the "critical" value, i.e., the value at which ionization and attachment probabilities are equal. This results from attachment lengths in a strongly electronegative gas being so small that electron currents can be maintained only if attachment is compensated by ionization; otherwise, net space charge could not be produced on short time scales. This physical condition is very much different from that for an air streamer [4], for which the attachment length is always large compared with streamer head dimensions so that streamer propagation becomes a question of energy balance in the head region. Even far below E_{cr}, a certain percentage of electrons will reach the anode, and net space charge continues to build up. As a consequence, air streamers propagate stably (without losing or gaining charge) at the so-called "stability field" (or "guiding field"), which is much less than the critical field.

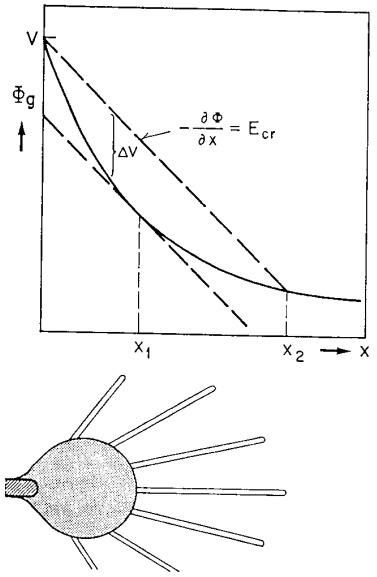

Figure 2 Illustration of the Streamer Mechanism in SF_6.
Top: applied potential (solid line), streamer head potential (upper dashed line), tangent to applied potential curve with slope E_{cr} (lower dashed line)
Bottom: resulting corona structure.

Based on these theoretical considerations, a qualitative explanation of corona development in SF_6 can be given (Figure 2). The solid line in Figure 2 is an example of the variation of the applied potential along the gap axis. The streamer rearranges the potential and field distribution such that the field in its track is roughly E_{cr}, which corresponds to the upper dashed line in Figure 2 with a slope of E_{cr}. Neglecting the effect of space charge deposited by the streamer, one expects the potential at some distance from the streamer to be the applied potential; for SF_6, this is not too bad an approximation. The potential drop between the streamer head (following the upper dashed line) and the surrounding gas (solid line) is responsible for avalanche growth in front of the head. As long as this potential drop increases in the course of propagation, subsequent avalanches are bigger than their predecessors and excess electrons are fed to the anode. The potential drop starts to decrease again after point x_1, where the applied field is E_{cr} (i.e., where the lower dashed line with slope E_{cr} is a tangent to the solid line). When the corona streamers have propagated to this point, the production of net space charge is essentially complete. Streamer propagation, however, continues until the voltage drop becomes zero (x_2), which is equivalent to stating that the average applied field in the streamer channel is the critical field. During the second phase of streamer propagation, the space charge is only redistributed.

The corona structure as derived from Schlieren photographs is sketched in the lower part of Figure 2 to show the correspondence of x_1 and the extension of the homogeneous zone on the one hand and of x_2 and streamer length on the other hand. The appearance of a homogeneous zone is believed to be caused by secondary processes (e.g. photoionization) leading to avalanches between streamer channels; this is only possible in the "critical volume" (with $E \geq E_{cr}$) bounded by x_1.

The improved understanding of corona development allows fairly precise predictions of corona size and charge, the latter being calculated under the assumption that within the critical volume the field is reduced to E_{cr} everywhere. Note that when comparing calculated and measured charges, corrections for the "apparent charge" have to be made, i.e., the image charges on the electrodes have to be taken into account. Figure 3 shows a comparison of measured (data points) and calculated (solid line) corona extensions (streamer lengths) as a function of V/E_{cr} for various gas compositions. For air/SF_6 mixtures, streamer propagation obeys the simple electrostatic conditions derived above down to below 1% SF_6 content [5]. The agreement between measured and calculated charges (Figure 4) is as satisfactory as that for corona extensions. Note that corona charges have an explicit pressure dependence.

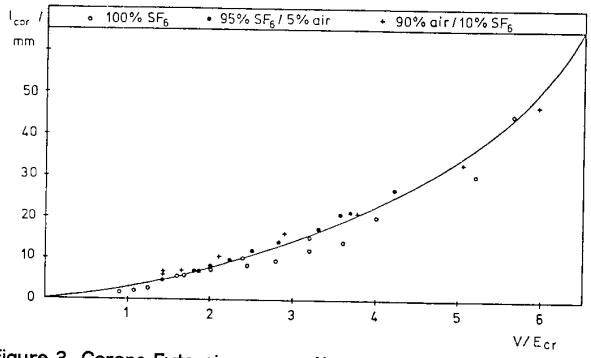

Figure 3 Corona Extension versus Normalized Voltage (V/E_{cr}) for Various Gas Mixtures. Gap geometry as in Figure 1; solid line is from the theory.

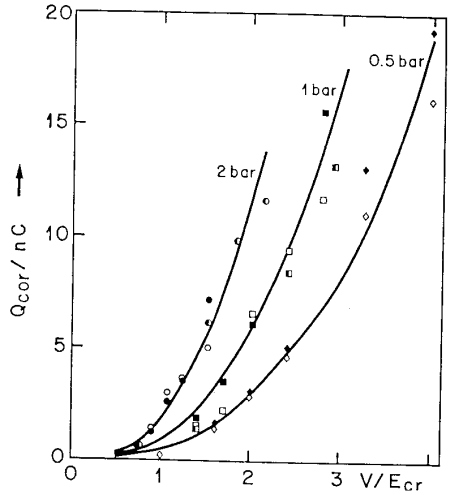

Figure 4 Apparent Corona Charge versus Normalized Voltage (V/E_{cr}) for Various Gas Mixtures. Gap Geometry as in Figure 1 and solid lines represent theory.

LEADER INCEPTION

The term "leader" is generally used for moderately conducting channels in gas discharges, without distinguishing among differing physical conduction mechanisms. The electric field in a leader

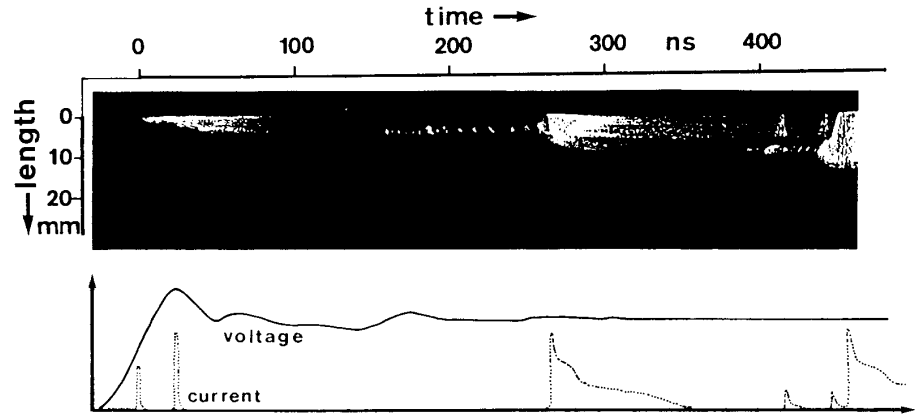

Figure 5 Fast Streak Record of Stepped Leader Propagation with Corresponding Voltage and Current Signals. Gap geometry as in Figure 1, with 200 kV and 1.5 bar pressure.

channel is much smaller than that of a streamer channel but still large compared to that of a spark. As in the case of the streamer, detailed studies of air leaders (e.g. [6]) have little relevance to strongly electronegative gases. In air, a leader is formed by heating a corona stem; leader propagation may be continuous or stepped, depending on the waveform. In SF_6, only stepped leaders have been observed, and the streamer to leader transition involves a novel phenomenon, for which the term "leader precursor" has been coined [2,3].

The general shape of breakdown curves for highly inhomogeneous field gaps, such as rod plane gaps, is well-known. The breakdown voltage first increases with pressure, reaches a maximum, then decreases with pressure, goes through a minimum, and finally increases nearly linearly with pressure (see Figure 13).

With fast rising pulses, the minimum tends to be very shallow. For pressures less than a "critical pressure", the corona inception voltage is smaller than the breakdown voltage, enabling partial discharges to exist. This effect is usually referred to as "corona stabilization" with the idea that the corona charge reduces the maximum field in the gap to below critical, thus preventing breakdown. In the following, we show that a totally different physical description is adequate, and the present study resolves past uncertainty concerning leader vs streamer breakdown.

From a number of fast streak records overlapping in time, a collage has been composed (Figure 5) to give an impression of the stepped propagation of a leader in SF_6. Voltage and current are displayed on the same time scale. After the corona expansion has stopped, a dark period is followed by renewed ionization activity at the corona boundary. The short channel at the boundary reilluminates fairly regularly and elongates asymmetrically in a few steps, i.e., the far end propagates into the gap in very small steps, whereas the anode directed end approaches the anode in large steps. Once the channel is connected to the anode, the potential at the far end is raised significantly, and generates new corona further into the gap. At this point of time, the channel experiences a rapid heating to dissociation temperature, which leads to a change in gas composition and density associated with a substantial reduction of the critical field (see later); the transition of the channel to the leader state is completed. As the discharge development described above always precedes this transition, the phenomenon is called "leader precursor". The same sequence of luminous events is observed in the subsequent leader steps, but with additional reilluminations of the leader channel in between steps.

The existence of the precursor finds a plausible explanation in terms of ion drift phenomena (Figure 6). As ionization and attachment coefficients are much greater than the net ionization coefficient in a strongly electronegative gas, a streamer channel will contain a large number of positive and negative ions but little net charge. After streamer propagation has stopped (at time 1 in Figure 6), the positive and negative ions start moving in opposite directions, thereby creating a net charge at the streamer tip (time 2). The corresponding increase in field strength leads to renewed ionization, which in turn augments the number of ions locally such that a dipolar charge distribution builds up (time 3). Finally, two field maxima move away from the streamer tip, in opposite directions and at different speeds, leaving a field just below critical in between (time 4). Electrostatic conditions make the propagation stop again, and a continuation is possible only after an expansion of the heated channel which results in a lowering of the critical field. Note that although the channel is heated, the temperature stays well below dissociation temperature.

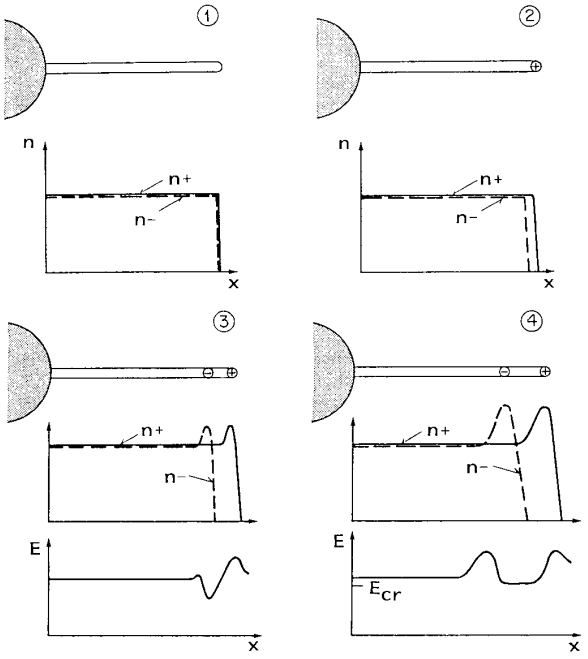

Figure 6 Illustration of Precursor Mechanism. (1) Ion density profiles after corona propagation. (2) Creation of net charge by ion drift. (3) Development of a dipolar charge distribution. (4) Propagation of ionization waves in opposite directions with E_{cr} in between.

The question of which parameters determine the leader inception (i.e., precursor inception) voltage must be addressed. From numerical simulations, the number density of ions in the streamer channel and the channel radius seem to be the most sensitive parameters. As the channel radius should depend mainly on gas pressure, one would expect to find a critical ion density that is a function of pressure only. The ion density is linked to corona charge or size in some way, and this is the point at which gap geometry becomes relevant, as shown below.

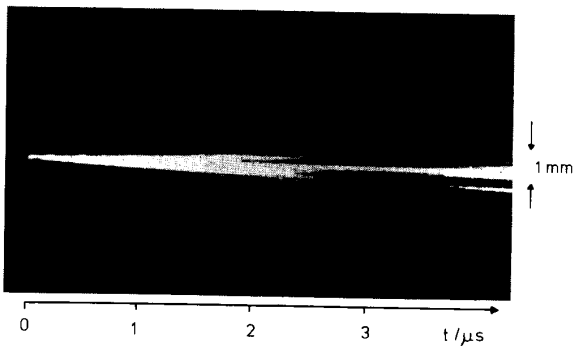

Figure 7 Shock Wave of Expanding Leader Channel (Schlieren streak record).

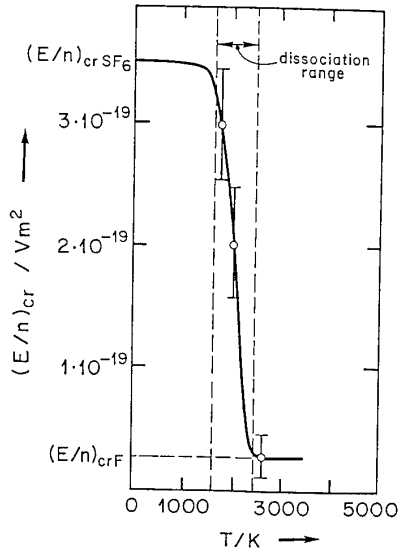

Figure 8 Reduced Critical Field of Hot SF_6 (LTE calculation)

LEADER PROPAGATION

The transition from the precursor to the leader state is associated with a considerable energy input, first because the total current of the leader corona is fed into the channel and secondly because the current pulse (Figure 5) has a slowly decaying tail and contains more charge than the current pulse of the first corona. The energy goes into heating and dissociation of the gas, with both processes leading to a large increase of pressure, since pressure is proportional to the product of particle density and temperature. The pressure increase is almost instantaneous so that a supersonic expansion of the channel occurs. Schlieren streak records, such as Figure 7, provide evidence for this shock wave. The temporal evolution of the gas density in the channel is obtained from a theoretical model [7]. The conduction mechanism in the leader channel is believed to be the same as that in the streamer channel, viz., a balance of attachment and ionization allows charge transport. The higher conductivity of the leader channel results from the lower gas density and the lower reduced critical field (Figure 8), which at high enough temperatures becomes the reduced critical field of atomic fluorine. Calculations of the leader field are in satisfactory agreement with measured average fields in the leader channel (Figure 9).

The relatively small voltage drop along the leader channel corresponds to a small difference between leader inception and leader breakdown voltages. Therefore a breakdown model need not perform a lengthy calculation for each leader step but need only compute the leader inception voltage and then add an approximate leader voltage drop.

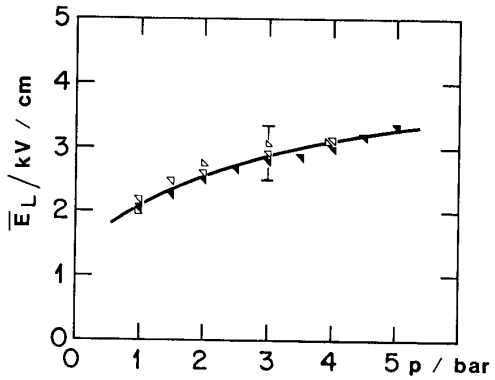

Figure 9 Average Field along the Leader Channel (Experimental values)

COMPUTER MODEL OF BREAKDOWN

The improved understanding of the relevant physical processes involved in discharge development lends itself to the formulation of a general breakdown model [1,8]. In doing so, the desire was to keep the model as simple as possible, consistent with demands for accuracy and wide applicability. Although based on physical principles throughout, the model contains empirical elements, in part because the quantitative theoretical description is still incomplete and in part because a much simpler treatment could be achieved without sacrificing accuracy.

Some restrictions imposed by the simplifications introduced into the model should be mentioned:

1) At present, the programs assume rotational symmetry, which is by no means a necessary restriction. In fact, the model has been successfully applied to three-dimensional cases by the authors.

2) The model is primarily useful for fast rising waveforms; if the rise time is of the order of tens of microseconds, field distortions resulting from ion drift may become important. As these are not included in the model, the predicted breakdown voltages can only be used as lower limits. The programs consider step pulse as well as lightning and switching impulse; the extension to other waveforms is trivial.

3) The theoretical treatment of the corona is based on the assumption that everywhere in the critical volume the field is reduced to the critical value. This condition is violated if the dimension of the critical volume in the direction of streamer propagation is much smaller than that in the direction perpendicular to propagation. Therefore the treatment of a thin wire to ground would be questionable in the framework of the model. Fortunately, this is not a severe restriction, as for the majority of practical applications of SF_6, the field is either quasihomogeneous, so that the breakdown voltage is determined by streamer inception (most GIS components), or the maximum stress occurs in a small spatial region, so that the model is applicable (particles in GIS, disconnect switch problems etc.)

4) Predicted breakdown voltages should be treated with some caution at pressures below 1 bar and gap lengths below 20 mm, as in these cases the approximations for the corona shape start to break down.

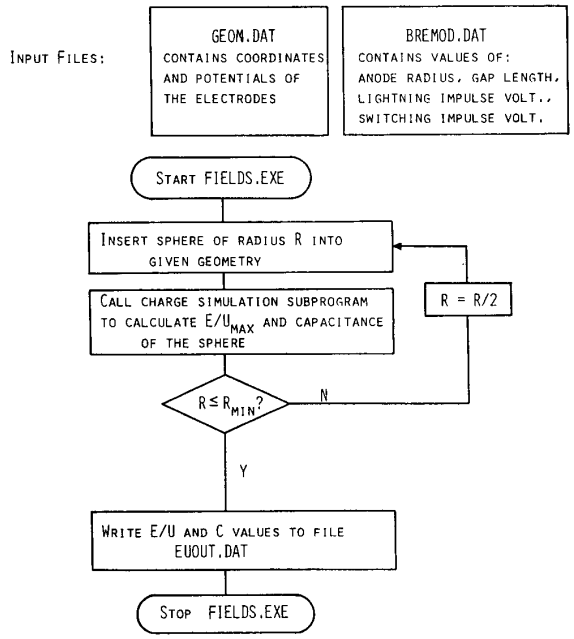

Figure 10 Flow Chart of Program FIELDS

Knowledge of field strengths is indispensable for the breakdown model. In order not to restrict the applicability to special cases, a numerical field calculation program capable of dealing with complicated gap geometries must be included. Here a surface charge simulation program [9] was used as a subprogram to the program FIELDS (Figure 10), which first calculates the maximum field at the anode and then inserts conducting spheres of various sizes into the geometry to simulate coronae. For each sphere, the maximum field and the capacitance of the sphere is stored in a file.

A second program, called BREMOD (Figure 11), then determines interpolation polynomials for the sphere capacitance and the per unit field as functions of the sphere radius and also determines the inverse functions. For a set of pressures, BREMOD calculates quantities required for the prediction of breakdown voltages, starting with the streamer inception voltage, which is computed in the simple approximation of Nitta and Shibuya [10]. Next comes an estimation of the streamer breakdown voltage that usually will be much higher than the leader breakdown voltage. The most important part of the program involves the determination of the leader inception voltage. As the numerical simulations of SF_6 streamers and precursors have not yet progressed sufficiently to predict the ion density, which is very likely to be the key parameter for leader inception, the tentative assumption is made that the ion density is related to the total corona charge. From a careful experiment, a set of "critical" corona charges has been determined once and is now used in all model calculations. (Note that a similar concept has been applied in a previous, qualitative model [11,12].) BREMOD searches for the voltage at which the corona charge is greater than or equal to the critical charge, starting at the streamer inception voltage. In this procedure, the corona size is calculated with a mathematical condition differing from the one described above but with practically identical results in the parameter range of practical interest. The leader arrival voltage is obtained by adding the leader voltage drop to the leader inception voltage. Finally the minimum breakdown voltage (equal to the step pulse breakdown voltage denoted by $U_{B\,DC}$ in Figure 11) is predicted by taking the minimum of streamer breakdown and leader arrival voltage.

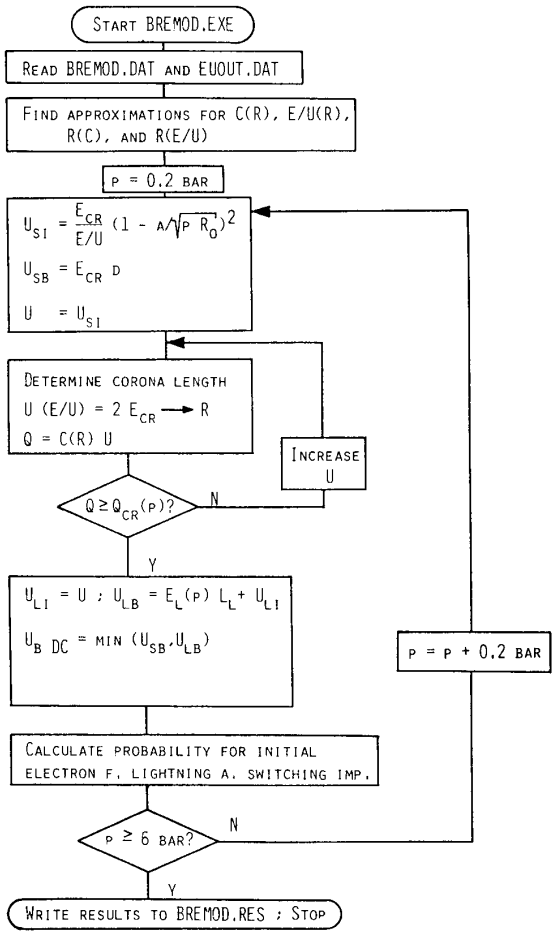

Figure 11 Flow Chart of Program BREMOD

One of the obvious applications of the breakdown model is the assessment during the design process of component withstand for test and in-service waveforms and tolerance to small defects, or – to put it the other way round – to assess the efficacy of test waveforms with respect to detection of defects. To this end, statistical effects must be assessed, as for practical switchgear, the probability of breakdown must be very small for the stresses expected in service, and an effective test waveform must have a reasonably high probability of detecting (by breakdown during a practical number of applications) a defect which represents a danger to in-service reliability. Therefore, one section of BREMOD is devoted to calculating the probability of having a "successful" initial electron. For the geometries that can be treated with the breakdown model, the integration in the modified volume time law could be simplified (see Paper II of this series). In a hemispherical region in front of the anode, the actual field distribution is replaced with that of a sphere (Figure 12), thereby reducing the volume integral to a one-dimensional integral and simplifying the determination of integration limits considerably. The integration in time starts as soon as the voltage exceeds the streamer inception voltage and stops when the voltage drops below the minimum breakdown voltage again. BREMOD gives breakdown probabilities for lightning and switching impulses of specified amplitudes.

$$W = 1 - \exp\left[-\int_{t_{min}}^{t_{max}} \int_{V_{cr}} \frac{dn_e}{dt}\left(1 - \frac{\eta}{\alpha}\right) dV\, dt \right]$$

a) integration in space

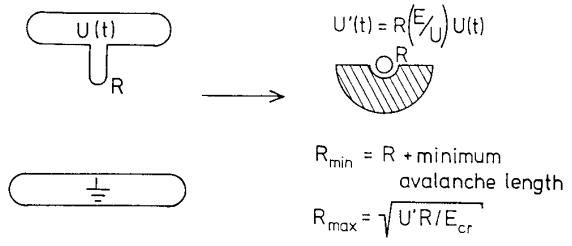

b) integration in time

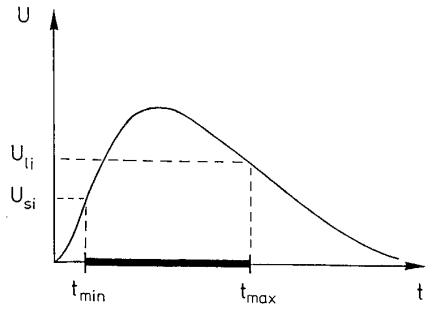

Figure 12 Calculation of the Probability Integral in Space (a) and Time (b).

COMPARISON OF MEASURED AND CALCULATED BREAKDOWN VOLTAGES

Thorough tests have been performed to check the accuracy and reliability of the computer breakdown model. In order to have separate tests for the statistical model and the leader model, various waveforms have been applied. The most suitable waveform for testing the leader model is a step pulse, because it practically eliminates the statistical variation of breakdown voltages. A total of 21 gap geometries have been investigated experimentally using step pulses. The field distribution ranged from strongly non-uniform (point-plane gaps) to nearly uniform (parallel plates with a small protrusion). Anode radii varied from 0.5 to 5 mm, gap lengths from 25 to 215 mm. In all cases, the agreement between predicted and measured breakdown curves was very good, with typical errors around 5%. Four examples are shown in Figure 13. Gap geometry #1 was a rod plane gap with a rod radius of 0.5 mm and a gap spacing of 37 mm, (negative) high voltage being applied to the plane electrode. Changing the gap distance to 65 mm results in the breakdown curve #11; #15 differs from #11 by replacing the rod with a sphere of 2.5 mm radius. Finally, #8 is a parallel plate gap with a rod of 0.5 mm radius protruding 3 mm from one plane. Although the breakdown curves in these examples differ greatly (rising or falling with pressure), they are equally well described by the breakdown model.

Figure 14 gives an example of one of several tests with lightning impulse [13]. The field distribution of this rod plane gap with a rod radius of 20 mm and a gap spacing of 80 mm is not strongly non-uniform. Therefore the minimum breakdown voltage does not depend critically on the accuracy of the leader model, i.e., one can test the statistical model alone. Using a polished electrode, the experimental breakdown voltages (dark shaded area) are in excellent agreement with prediction (solid line). With a rough electrode, a bend in the breakdown curve is observed (light shaded area), which can be reproduced with the model, if the surface roughness is simulated with small spheres assumed to be fixed to a perfect electrode surface (broken line). From these comparisons, the adequacy of the statistical model for practical problems becomes evident. Further checks for more complex geometries are provided in [1].

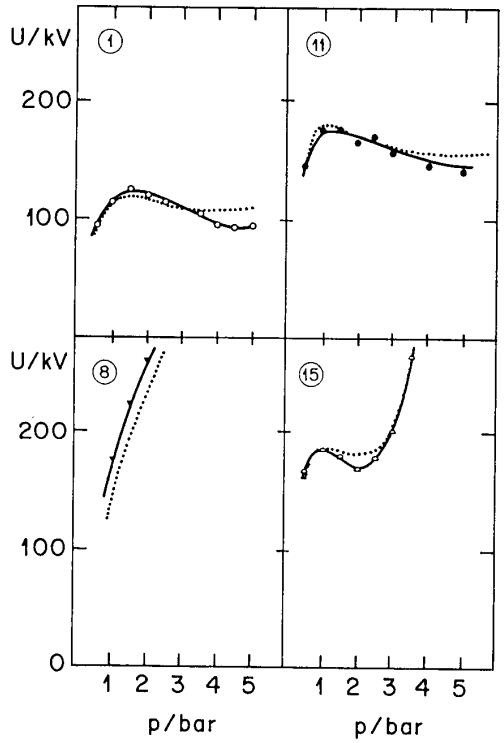

Figure 13 Comparison of Measured (solid lines) and Calculated (dotted lines) Breakdown Curves for Various Gaps for Step Pulse Application.

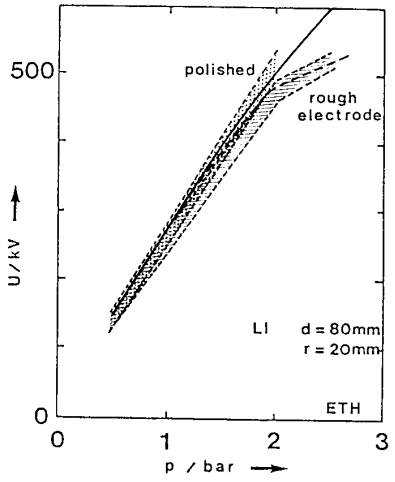

Figure 14 Comparison of Measured (shaded areas) and Calculated (solid and dashed lines) Lightning Impulse Breakdown Curves for a Rod Plane Gap (diameter 40 mm; spacing 80 mm) with Polished and Rough Electrodes.

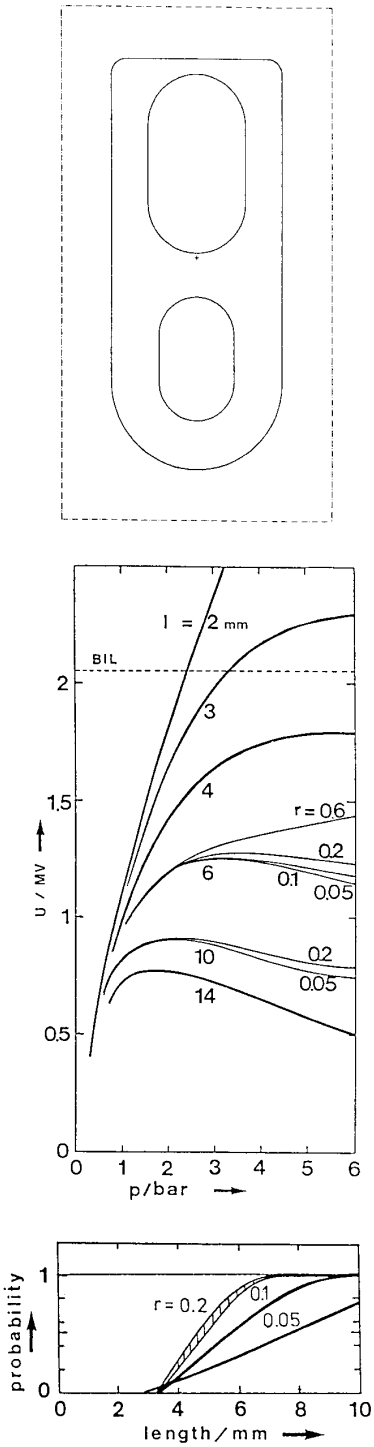

Figure 15 Application of the Breakdown Model to the Case of Fixed Particles in GIS.
a: Three electrode arrangement; particle position marked with a cross.
b: Predicted step pulse breakdown curves.
c: Breakdown probability as a function of particle length for various particle radii (lightning impulse of 2100 kV)

APPLICATIONS TO PRACTICAL PROBLEMS

Even though the present computer model is subject to some restrictions, a multitude of practical applications is obvious: Particle-related problems in gas insulated switchgear, radial and axial breakdown in disconnectors, cold gas withstand capability of circuit breakers, complex electrode shapes in medium high voltage equipment, etc. can all be treated in the framework of the model. In fact, the model is now being applied to component design.

The following example deals with the problem of conducting particles in GIS, a problem that has often been tackled experimentally in the past. Obviously the possibility of predicting the effect of particle contamination should have a beneficial effect on both design cost and component reliability. In this example, the deterioration of the withstand capability of an open disconnector resulting from the presence of a conducting particle is simulated. Figure 15a gives the model geometry, which is a simple three electrode arrangement with a "particle" of variable length and radius (hemispherically capped rod) attached to one electrode at the point of maximum stress. The predicted step pulse breakdown voltages (Figure 15b) illustrate the gradual transition from a Paschen law type breakdown curve to a typical leader breakdown curve with increasing particle length. For a step pulse, the particle radius is of lesser influence, as long as the particle is "slim", i.e. much longer than wide. The radius is, however, important in determining the critical volume and, therefore, the statistical time lag. For a lightning impulse test at 2100 kV, breakdown probabilities have been calculated as a function of particle length for several particle radii (Figure 15c). A fixed particle of 4 mm length and 0.1 mm radius would be detected with a probability of about 20% in such a the test. On the other hand, the minimum breakdown voltage with this particle of more than 1.7 MV at typical operating pressure provides a sufficient safety margin with respect to the AC peak voltage. Thus the lightning impulse test is seen to be a reasonable test of component reliability as far as a fixed particle is concerned.

CONCLUSIONS

Extensive studies of discharge development in SF_6 and their interpretation in terms of physical processes have provided the basis for a quantitative computer breakdown model. With the inclusion of a statistical model of initial electron production (cf. Part II), the predictive capability of the computer breakdown model is such that for the majority of practical applications, SF_6 breakdown voltages can be calculated with a typical error of 5%.

The predictability of insulating strength is expected to have a considerable impact on component design, especially where the field is not quasi-homogeneous (disconnectors, circuit breakers etc.), in particular for complex three-dimensional electrode arrangements (three phase encapsulation in GIS, medium high voltage equipment). In principle, reliability should increase and development cost should decrease.

From both the utilities' and the manufacturers' point of view, a quantitative breakdown model also means a step forward in developing an adequate testing philosophy for GIS. In the above example, the efficacy of existing test procedures could be easily assessed. Other situations, such as the presence of free particles, require a more refined treatment, because, for example, in an AC bias lightning test additional effects such as particle bouncing and spatial and temporal variations of ion density [14] must be considered simultaneously. The problem of optimizing test procedures is still far from being solved; however, in providing objective criteria of assessment, the breakdown model is a valuable tool for further work.

Future studies similar to those reported here will be necessary to remove some restrictions presently imposed on the model. To the present, only breakdown under positive polarity has been investigated extensively. Although negative leader inception voltages are roughly twice those for positive polarity, situations may occur in which this is compensated by the fact that initial electrons are more readily available with negative polarity. A

second meaningful extension would be the inclusion of ion drift effects on time scales typical of switching impulse or AC application. Finally physical effects with waveforms characterized by a substantial voltage variation during leader propagation (fast transients, oscillating lightning impulse, etc.) should be studied to complete the knowledge of practically relevant discharge phenomena.

REFERENCES

1. Wiegart, N. and F. Pinnekamp. "Corona Stabilization to the Testing of Gas-Insulated Switchgear" Final Report of Canadian Electrical Association Contract 153 T 310; Available from The Canadian Electrical Association, Suite 580, One Westmount Square, Montreal, Quebec, H3Z 2P9

2. Gallimberti, I. and N.J. Wiegart. "Streamer and Leader Formation in SF_6 and SF_6 Mixtures under Positive Impulse Conditions, Part I/Part II" 8th International Conference on Gas Discharges and their Applications, Oxford, 1985.

3. Gallimberti, I. and N.J. Wiegart "An Investigation of the Streamer to Leader Transition and Related Phenomena in SF_6 and SF_6 Mixtures Under Positive Impulse Conditions" to be published, 1986.

4. Gallimberti, I. "A Computer Model for Streamer Propagation". J. Phys. D: Appl. Phys. 5, 2179-2189, 1985.

5. Gallimberti, I, G. Marchesi and R. Turri. "Corona Formation and Propagation in Weakly or Strongly Attaching Gases." 8th International Conference on Gas Discharges and their Applications Oxford, 1985.

6. Gallimberti, I. "The Mechanism of the Long spark Formation." Journal de Physique, Colloque C7, supplement au no. 7 40 C7-193 - C7-250, 1979.

7. Niemeyer, L. "A Model of SF_6 Leader Channel Development." 8th International Conference on Gas Discharges and their Applications, Oxford, 1985.

8. Wiegart, N.J. "A Semi-Empirical Leader Inception Model for SF_6." 8th International Conference on Gas Discharges and their Applications, Oxford, 1985.

9. Sato, S. and B. Bachmann. "A Three Dimensional High Speed Surface Charge Simulation Method (3D-HSSSM)." 4th ISH Athens, paper 11.08, 1983

10. Nitta, T. and Y. Shibuya "Electrical Breakdown of Long Gaps in Sulfur Hexafluoride." IEEE Trans. PAS-90, 1065-1071, 1971.

11. Niemeyer, L. and F. Pinnekamp "Leader Discharges in SF_6." J. Phys. D: Appl. Phys. 16, 1031-1045, 1983.

12. Pinnekamp, F. and L. Niemeyer "Qualitative Model of Breakdown in SF_6 in Inhomogeneous Gaps" J. Phys. D: Appl. Phys., 16, 1293-1302, 1983

13. Schmid, R. private communication, 1985

14. Boggs, S.A. and N. Wiegart "Influence of Experimental Conditions on Dielectric Properties of SF_6-Insulated Systems - Theoretical Considerations." Gaseous Dielectrics IV, L. Christophorou, ed. Pergamon, 1984.